American Mineralogist, Volume 93, pages 902–909, 2008

Rudashevskyite, the Fe-dominant analogue of sphalerite, a new mineral: Description and crystal structure

Sergey N. Britvin,[1,*] Alla N. Bogdanova,[2] Maya M. Boldyreva,[3] and Galina Y. Aksenova[4]

[1]Department of Crystallography, St. Petersburg State University, Universitetskaya Nab. 7/9, 199034 St. Petersburg, Russia
[2]Geological Institute, Kola Science Center, Russian Academy of Sciences, Fersman Str. 21, 184200 Apatity, Russia
[3]Department of Mineral Deposits, St. Petersburg State University, Universitetskaya Nab. 7/9, 199034 St. Petersburg, Russia
[4]Mekhanobr-Engeneering Join-Stock Company, Vasilievsky ostrov, 21 line 2, 199026 St. Petersburg, Russia

Abstract

Rudashevskyite, Fe-dominant analogue of sphalerite, is an accessory phase in the Indarch meteorite (enstatite chondrite, EH4). It occurs as xenomorphic polycrystalline grains, 5–120 μm in size, associated with clinoenstatite, kamacite, troilite, oldhamite, niningerite, schreibersite, and roedderite. Macroscopically, rudashevskyite is black with resinous luster. In reflected light, it is gray with brownish tint. Isotropic, no internal reflections. Reflectance in air (%, λ): 19.5(400), 19.5(420), 19.5(440), 19.5(460), 19.6(470), 19.8(480), 19.8(500), 19.9(520), 20.2(540), 20.3(546), 20.5(560), 20.7(580), 20.8(589), 20.9(600), 20.9(620), 21.1(640), 21.1(650), 21.1(660), 21.1(680), and 21.2(700). Brittle. D_c 3.79 g/cm^3. VHN 353 kg/mm^2. Chemical composition (electron microprobe, average of 31 analyses on 11 grains, wt%): Fe 37.1, Zn 24.7, Mn 2.4, Cu 0.4, S 35.3, total 99.9. Empirical formula (2 apfu): $(Fe_{0.61}Zn_{0.35}Mn_{0.04}Cu_{0.01})_{\Sigma=1.00}S_{1.00}$, ideally (Fe,Zn)S. Cubic, $F\bar{4}3m$, a 5.426(2) Å, V 159.8 (2) Å^3, Z = 4. X-ray powder diffraction pattern (Debye-Scherrer, Fe$K\alpha$), [d(*I*)(*hkl*)]: 3.130(100)(111), 2.714(10)(200), 1.919(50)(220), 1.634(40)(311), 1.359(5)(400), 1.246(30)(331), 1.107(30)(422), 1.045(30)(511, 333). Crystal structure: R_1 = 0.050 for 26 unique observed ($|F_o| \geq 4\sigma_F$) reflections. It is named in honor for N.S. Rudashevsky, St. Petersburg, Russia, for his contributions to the study of ore minerals.

Keywords: Rudashevskyite, new mineral, sphalerite, wurtzite, FeS, meteorite, enstatite chondrite, black smokers

Introduction

Sphalerite and wurtzite, polytypes of ZnS, are common minerals in various geological occurrences. Their synthetic Fe-dominant analogues are well known and are chemically and structurally studied by several authors. Natural (Fe,Zn,Mn)S minerals were originally described from meteorites. Paul Ramdohr (Ramdohr 1963, 1973) was the first who optically characterized (Fe,Zn)S sulfide (*Mineral K*) in the Indarch meteorite (enstatite chondrite, EH4). Further investigations revealed that Fe-dominant members of (Fe,Zn,Mn)S solid solutions are typical accessory minerals in enstatite chondrites (Buseck and Holdsworth 1972; Kissin 1986, 1989; Rambaldi et al. 1986; El Goresy and Ehlers 1987, 1989; El Goresy et al. 1988; Kimura 1988; Ikeda 1989; Lin et al. 1991; Zhang and Sears 1996; Lin and Kimura 1997, 1998; Petrichenko and Ulyanov 1998; Lin and El Goresy 2002; Lorenz et al. 2003). These minerals were also described from three iron meteorites (octahedrites) related to the IAB group: Odessa, Waterville and Burkhala (El Goresy 1967; Weinke et al. 1977; Yaroshevsky et al. 1989). Unfortunately, meteoritic occurrences of (Fe,Zn,Mn)S sulfides were not supported by either X-ray or TEM data, thus their relationship to sphalerite or wurtzite remained unsolved.

Terrestrial occurrences of Fe-dominant (Fe,Zn,Mn)S minerals include hydrothermal sulfide assemblages of black smokers in oceanic rift zones (Izawa et al. 1991; Peter and Scott 1988; Lawrie and Miller 2000; Glasby and Notsu 2003) and natrocarbonatite lavas of Oldoinyo Lengai volcano, Tanzania (Mitchell and Belton 2004).

In this article, we present a description of properties and structure refinement of the Fe-dominant analogue of sphalerite, based on a material from the Indarch meteorite (*Mineral K* of Ramdohr 1963, 1973). The new mineral is named rudashevskyite, in honor of Nickolay S. Rudashevsky (1944–), St. Petersburg, Russia, for his contributions to study of ore minerals. Both the mineral and its name have been approved by the Commission on New Minerals and Mineral Names, International Mineralogical Association. The type specimen of rudashevskyite is deposited at the Mineralogical Museum, Department of Mineralogy, St. Petersburg State University, St. Petersburg, Russia.

Rudashevskyite in Indarch

The enstatite chondrite Indarch, EH4, is a long known (fall witnessed 1894) and well-studied representative of its group. Like other low-metamorphic grade enstatite chondrites, the fine-grained matrix and chondrules of Indarch consist of clinoenstatite, with subordinate sodium-rich plagioclase, tridymite, and roedderite. The principal opaque minerals are represented

* E-mail: sbritvin@gmail.com

by Si-bearing kamacite, troilite, and schreibersite. Less common opaque minerals include graphite, niningerite, oldhamite, daubreelite, djerfischerite, and Na-H_2O-bearing Cr-sulfide (Brearley and Jones 1998).

Rudashevskyite is an accessory mineral in Indarch. In total, we observed 19 grains scattered over an area of approximately 0.5 cm^2. It occurs as xenomorphic grains, 5–150 μm in cross-section, their segregations filling interstices between the crystals and grains of adjacent minerals in the matrix of chondrite. The grains are randomly disseminated among associated minerals, both silicates and opaque minerals. We never observed rudashevskyite in the chondrules of the meteorite. In reflected light, core parts of rudashevskyite aggregates look homogeneous, whereas boundary regions contain abundant troilite patches (Fig. 1). Since the first optical description of this sulfide by Ramdohr (*Mineral K*; Ramdohr 1963, 1973), several authors have studied its chemical composition by means of the electron microprobe (Kissin 1986, 1989; El Goresy and Ehlers 1987, 1989). They first observed unusual lamellar and porous textures, compositional zoning and exsolution lamellae of troilite in the aggregates of the mineral. BSE photographs with enhanced contrast reveal fine foliated structures composed of thin subparallel lamellae (Fig. 2). The thickness of individual lamellae is usually 2–3 μm (Fig. 3a), but in some cross-sections may reach 6–7 μm. This kind of lamellar aggregate with lenticular pores between lamellae was called "porous structures" (El Goresy and Ehlers 1987, 1989; Kissin 1989). According to El Goresy and Ehlers (1987, 1989), the origin of the pores may be attributed to release of elemental sulfur caused by probable sphalerite-wurtzite inversion. Another explanation, however, is that these pores are interlamellar boundaries formed during growth of rudashevskyite aggregates.

PHYSICAL AND OPTICAL PROPERTIES

Macroscopically, rudashevskyite grains (30–100 μm) extracted from meteorite matrix are black with resinous to submetallic luster. The mineral is brittle, and its powder is brown-black. No distinct cleavage was observed, obviously due to polycrystalline

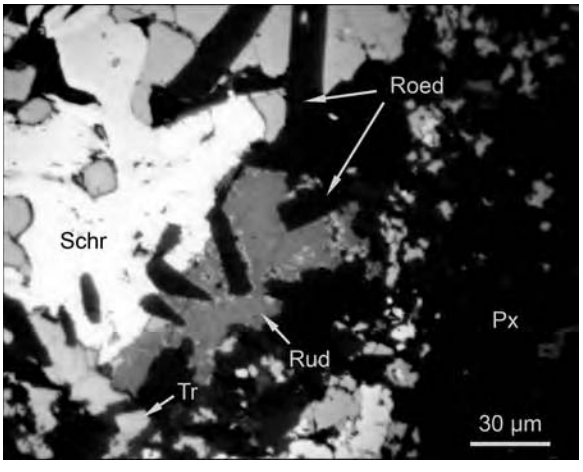

FIGURE 1. Xenomorphic grain of rudashevskyite (Rud) attached to large schreibersite grain (Schr), associated with troilite (Tr), idiomorphic roedderite tablets (Roed), and clinoenstatite (Px). Note abundant micropatches of troilite along rudashevskyite rim. Reflected light.

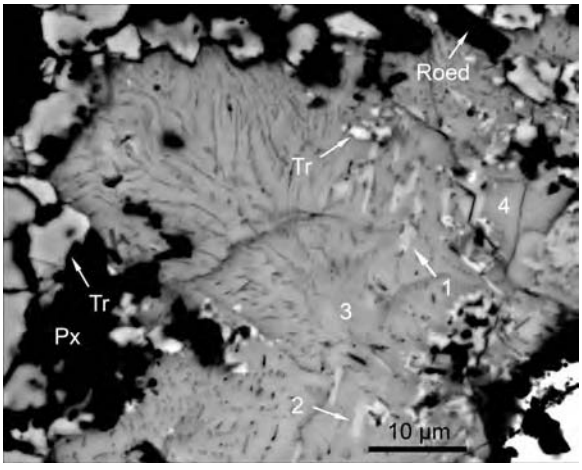

FIGURE 2. Foliated lamellar aggregate of rudashevskyite (Rud) with inclusions of troilite (Tr), associated with roedderite (Roed) and clinoenstatite (Px). Brighter lamellae are slightly enriched in Zn (~0.03 Zn apfu). Numbers correspond to analyses listed in Table 2. BSE image.

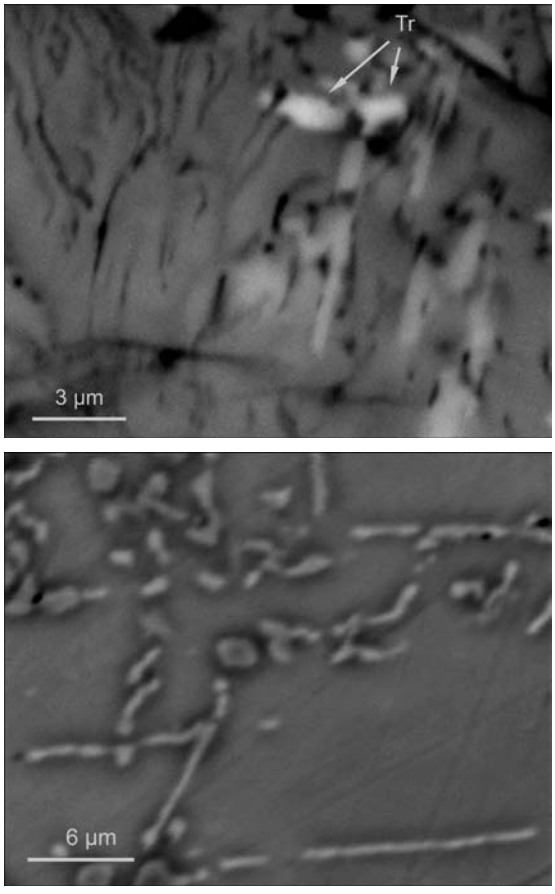

FIGURE 3. (**a**) Detail of Figure 2 showing relative brightness of troilite (Tr) lamellae in BSE compared with rudashevskyite (dark and light lamellae). Note that troilite looks brighter than rudashevskyite. (**b**) Exsolution lamellae of troilite (light) in sphalerite, $(Zn_{0.60}Fe_{0.35}Mn_{0.06})_{\Sigma=1.01}S_{0.99}$ (dark matrix), meteorite Sardis (IAB). BSE image. Note that both rudashevskyite and sphalerite look darker than troilite despite greater mean atomic number.

nature of the aggregates. Average micro-indentation hardness measured with Vickers pyramid (20 g load) is 353 kg/mm^2, ranging between 313 and 383 kg/mm^2 for five measurements, a value noticeably higher than VHN of sphalerite (208–224 kg/mm^2, Criddle and Stanley 1993). Calculated density for the average composition, $(Fe_{0.61}Zn_{0.35}Mn_{0.04}Cu_{0.01})_{\Sigma=1.00}S_{1.00}$, is 3.79 g/cm^3.

In reflected light rudashevskyite is gray with distinct brownish tint. It is isotropic and has no internal reflections. Reflectance values have been measured in air (for point no. 4 on Fig. 2) by means of an MSP-10 spectrophotometer (LOMO, St. Petersburg), using a 40× objective of 0.65 numerical aperture, with 3 μm spot diameter and SiC (Carl Zeiss no. 545) as reference standard. They are listed in Table 1 in comparison with data for synthetic Fe-rich sphalerite (Chvileva et al. 1988) and our data for Fe-Mn-rich sphalerite from the Sardis meteorite. Color values for both rudashevskyite and sphalerite were calculated by means of MicroMin software (Boldyreva et al. 2002), relative to the CIE recommended illuminants C and A with color temperature of 6774 and 2856 K, respectively (Table 1). The considerably different dominant wavelength λ_d, orange-yellow (582–589 nm) for rudashevskyite and greenish-blue (473–488 nm) for sphalerite, is responsible for the tint of the minerals in reflected light. Rudashevskyite possesses higher luminance (Y, %) and lower excitation purity (P_e, %), relative to the illuminant C.

The reflectance curve of rudashevskyite is presented in Figure 4, in comparison with reference values for sphalerites of different composition. Full data for pure sphalerite-type FeS are not available, but Murowchick and Barnes (1986) measured its reflectance at 580 nm. This value, 28(1)%, can be used for comparison with corresponding data for other minerals of the series. These values are plotted against Fe content (apfu) (Fig. 4).

TABLE 1. Reflectance values of rudashevskyite and sphalerite measured in air

λ (nm)	*R* (%)		
	Rudashevskyite	Sphalerite*	Sphalerite*,†
400	19.5	19.9	–
420	19.5	19.4	20.4
440	19.5	19.0	19.6
460	19.5	18.5	19.1
470	19.6	18.4	18.8
480	19.6	18.3	18.4
500	19.8	18.0	18.2
520	19.9	17.9	18.0
540	20.2	17.8	17.8
546	20.3	17.8	17.6
560	20.5	17.7	17.5
580	20.7	17.6	17.3
589	20.8	17.6	17.2
600	20.9	17.6	17.2
620	20.9	17.5	17.2
640	21.1	17.4	17.2
650	21.1	17.3	20.4
660	21.1	17.3	19.6
680	21.1	17.2	19.1
700	21.2	17.2	18.8
CIE color values: illuminant C (6774 K)			
x	0.313	0.305	0.301
y	0.318	0.309	0.306
Y (%)	21.4	17.7	17.9
λ_d	585	473	476
P_e (%)	1.2	2.8	4.4
CIE color values: illuminant A (2856 K)			
x	0.450	0.443	0.440
y	0.408	0.405	0.404
Y (%)	21.5	17.7	17.7
λ_d	592	486	488
P_e (%)	2.0	1.1	1.9

* Sardis meteorite, $(Zn_{0.60}Fe_{0.35}Mn_{0.06})_{1.01}S_{0.99}$, our data.
† Synthetic, 45 mol% FeS, Chvileva et al. (1988).

CHEMICAL COMPOSITION

Chemical composition of rudashevskyite from Indarch has been previously studied in context of its use as a geothermometer (Kissin 1986, 1989; El Goresy and Ehlers 1987, 1989). Our microprobe data were obtained with a LINK AN10000 EDS system operated at 20 kV, 1 nA beam current, with 1–3 μm estimated beam diameter, 150 s counting time per spot, using the following standards: pyrite (for Fe), synthetic ZnS (Zn and S), Cu and Mn metals (Cu and Mn), and GaAs (Ga). Selected analyses for 11 different grains are given in Table 2. No other elements with atomic number greater than 11 (Na) were detected. Special care has been taken to prove the absence of Mg, Ca, and Ga. These elements were checked with a Microspec WDX wavelength dispersive spectrometer (20 kV accelerating voltage, 25 nA beam current). We could not find detectable (>0.05 wt%) contents of Ca, Ga, or Mg in analyzed grains. Kissin (1989) reported up to 1.6 wt% Ga in the mineral from Indarch, whereas El Goresy and Ehlers (1989) found less than 0.1 wt%. Magnesium was reported by Nagel et al. (1989) as a major element in sphalerite from enstatite chondrites. Later, this abstract was cited by El Goresy and Ehlers (1989) with respect to the mineral from Indarch. Unfortunately, the abstract by Nagel et al. (1989) is not supported by their analytical data. Further analyses (El Goresy and Ehlers 1989; Kissin 1989) do not show detectable amounts of Mg in rudashevskyite, in agreement with our results.

In addition to analysis for elements with *Z* greater than 11, we performed special measurements for nitrogen and carbon.

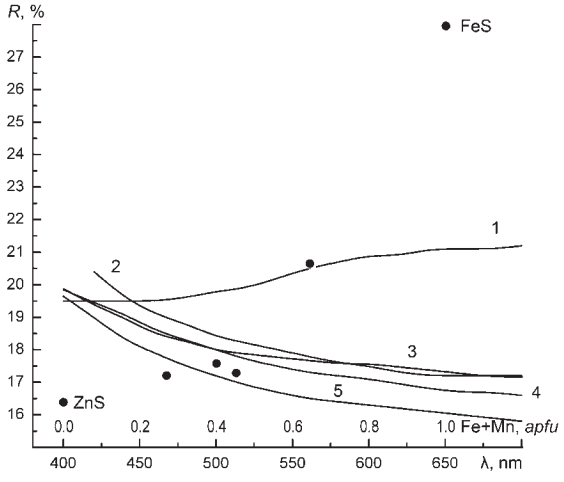

FIGURE 4. Reflectance spectrum of rudashevskyite measured in air, curve (1), in comparison with spectra of reference sphalerites: (2) 45 mol% FeS (Chvileva et al. 1988); (3) Sardis meteorite, $(Zn_{0.60}Fe_{0.35}Mn_{0.06})_{\Sigma=1.01}S_{0.99}$ (our data); (4) 23 mol% FeS (Criddle and Stanley 1993); (5) ZnS with 0.4 wt% Cd (Criddle and Stanley 1993); outer bottom scale in nanometers. Black circles represent reflectance values measured at 580 nm for above mentioned minerals and for pure sphalerite-type FeS (Murowchick and Barnes 1986); inner bottom scale in atoms per formula unit.

TABLE 2. Chemical composition of rudashevskyite from Indarch meteorite

Wt%						Formula amounts (2 apfu)					Ref.	Comment
Fe	Zn	Mn	Cu	S	Total	Fe	Zn	Mn	Cu	S		
33.9	27.8	2.3	0.5	35.3	99.8	0.56	0.39	0.04	0.01	1.01	1	70 (1)*
33.7	28.5	2.1	0.4	34.4	99.1	0.56	0.40	0.04	0.01	0.99	1	70 (2)
36.1	26.7	1.6	0.0	34.6	99.0	0.60	0.38	0.03	0.00	1.00	1	70 (3)
36.5	26.0	1.8	0.4	35.1	99.8	0.60	0.36	0.03	0.01	1.00	1	70 (4)†
36.5	26.8	2.4	0.5	34.3	100.5	0.60	0.38	0.04	0.01	0.98	1	30
37.4	23.2	2.9	0.4	36.4	100.3	0.60	0.32	0.05	0.01	1.02	1	35
37.9	23.2	3.0	0.3	35.6	100.0	0.62	0.32	0.05	0.00	1.01	1	40
39.9	20.9	2.9	0.5	35.9	100.1	0.65	0.29	0.05	0.01	1.01	1	30
35.8	26.1	3.6	0.6	34.6	100.7	0.58	0.36	0.06	0.01	0.98	1	20
42.4	20.9	2.2	0.3	35.7	101.5	0.68	0.29	0.04	0.00	1.00	1	50
40.2	20.8	2.4	0.3	36.0	99.7	0.65	0.29	0.04	0.00	1.02	1	50
37.4	22.9	2.7	0.6	35.4	99.0	0.61	0.32	0.05	0.01	1.01	1	70
33.8	29.4	1.7	0.4	35.1	100.4	0.55	0.41	0.03	0.01	1.00	1	70
37.8	22.8	2.6	0.5	36.2	99.9	0.61	0.32	0.04	0.01	1.02	1	40
31.4	23.5	2.88	<0.05	34.3	92.15	0.54	0.34	0.05	0.00	1.01	2	Cr 0.07 wt%
32.6	27.0	2.55	0.50	34.3	96.95	0.55	0.39	0.04	0.01	1.01	2	
32.5	24.2	3.37	0.21	34.6	94.88	0.55	0.35	0.06	0.00	1.03	2	Ga 0.09 wt%
39.34	23.02	2.45	–	35.26	100.07	0.64	0.32	0.04	–	1.00	3	
35.89	25.10	2.40	–	35.14	98.91	0.59	0.35	0.04	–	1.01	3	Ga 0.38 wt%
34.54	22.46	3.28	–	36.13	97.02	0.57	0.32	0.06	–	1.04	3	Ga 0.61 wt%
41.21	20.34	1.75	–	34.02	98.13	0.69	0.29	0.03	–	0.99	3	Ga 0.81 wt%
32.73	26.19	2.03	0.75	35.37	98.58	0.54	0.37	0.03	0.01	1.02	3	Ca 0.80; Ga 0.71

Notes: References: 1 = our data; 2 = El Goresy and Ehlers (1989); 3 = Kissin (1989). A dash denotes not sought.
* Grain size in micrometers. Numbers in parentheses correspond to point numbers on Figure 2.
† Grain used for reflectance measurements.

For this purpose, a section of meteorite was cut and then polished by diamond powders, using CFC-113 (ClF_2C-$CFCl_2$) as liquid medium. No impregnation by epoxy was performed, to minimize possible contamination. Analyses for N and C were carried out using LINK ISIS EDS system (15 kV, 3 nA) on the sections coated with 20 Å gold film. Nitrogen was not detected, but the intensity of N*K*α excitation is low, therefore we cannot exclude 0.*n* wt% of nitrogen in the composition of the mineral. Carbon was always detected at the levels of 0.*n* wt%, but both on rudashevskyite and troilite areas. As a consequence, surface contamination is rather possible.

As seen in Table 2, the chemical composition of rudashevskyite varies widely, between 55 and 68 mol% of FeS. We could not find a correlation between grain size and composition. Individual grains of rudashevskyite from Indarch possess some characteristic features that can be observed in BSE images with enhanced contrast (Figs. 2 and 3a). As first found by El Goresy and Ehlers (1987), aggregates of the mineral always contain lamellae, which look brighter in BSE than surrounding rudashevskyite. Analyses of these lamellae (points 1 and 2 on Fig. 2) are presented in Table 2 (numbers in parentheses). The lamellae are slightly enriched in Zn, by ~2 wt% (0.02–0.04 Zn apfu), as compared with composition of main part of the aggregate (points 3 and 4 on Fig. 2). Note that rudashevskyite grains appear darker in BSE than adjacent troilite (Fig. 3a), whereas the mean atomic number, MAN, of rudashevskyite (21.5–21.8) is greater than MAN of troilite (21.0). It is usually accepted that the greater the MAN the brighter BSE image of the corresponding phase. To find an explanation for the discrepancy observed in rudashevskyite-troilite intergrowths, we also conducted BSE and composition study of sphalerite-troilite intergrowths from the Sardis meteorite (coarse octahedrite, IAB). Sphalerite from our sample of Sardis, $(Zn_{0.60}Fe_{0.35}Mn_{0.06})_{\Sigma=1.01}S_{0.99}$, has a composition similar to that reported by Schwarcz et al. (1975). Despite that MAN of this sphalerite is even greater than that of rudashevskyite, the mineral is still darker in BSE than troilite (Fig. 3b). This observation can be explained by the fact that both sphalerite and troilite have different but close MAN's, whereas the density of troilite (D_x 4.85 g/cm^3) is considerably greater than the density of rudashevskyite and even of sphalerite (for pure sphalerite, D_x 4.10 g/cm^3). The fact that relative BSE brightness is different for different polymorphs of the same substance and is dependent on density is noted by several authors (see, for instance, Chen et al. 2003). In the case of sphalerite-rudashevskyite-troilite, we observe similar dependence for the phases with different composition.

CRYSTAL STRUCTURE AND CRYSTALLOGRAPHY

For purposes of structure refinement, an 80 × 100 μm grain of rudashevskyite was recovered from the polished section and mounted on a glass fiber. Data collection was performed by means of a two-circle Stoe IPDS II image plate diffractometer operated at 50 kV and 40 mA, using monochromatized Mo*K*α radiation. Preliminary study of a few frames recorded from the grain showed that it is not a single crystal but a polycrystalline aggregate; therefore the grain was broken into smaller ones. A 20 × 30 × 30 μm fragment was than selected for data collection. In total, 90 frames were collected, with framewidths of 2° in ω, exposure time 180 s per frame, 100 mm detector-to-crystal distance. Subsequent data processing was performed using the Stoe X-Area software package (Stoe and Cie GmbH 2005). Initial examination of collected frames revealed poor quality of the pattern with smeared diffraction peaks. First attempts to index the reflections showed that the broken fragment was still a polycrystalline aggregate. To distinguish between the patterns related to single-crystal domains, we used the following scheme of indexing. After the first single-crystal domain had been indexed, all diffraction peaks related to it were removed from the total pattern, followed by subsequent indexing of the remaining peaks, and so on. Finally, three independent domains were extracted, each of them corresponding to an *F*-centered cubic cell with an

edge close to that expected for sphalerite. Diffraction peaks remaining after removal of rudashevskyite reflections displayed the pattern corresponding to an *I*-centered cubic cell with *a* exactly matching that of kamacite. No peaks were observed that might belong to either troilite or pyrrhotite. The data for each of four domains were corrected for Lorentz, polarization, absorption and background effects. Structure refinement was carried out against F^2 using SHELXL-97 (Sheldrick 1997). Details on data collection, unit cell determination and structure refinement are listed in Table 3, along with isotropic displacement parameters obtained by refinement. Supplementary reflection data (*.hkl and *.cif files) are deposited with MSA[1]. The structure of each rudashevskyite domain has been refined in space group $F\bar{4}3m$, with parameter *a* of 5.426(2) Å obtained from powder data, confirming its sphalerite structure arrangement: (Fe,Zn) in 4*a* (0,0,0), S in 4*c* (¼,¼,¼), with (Fe,Zn)-S bond length of 2.350(1) Å. Data obtained for kamacite were processed in space group $Im\bar{3}m$ yielding Fe in 2*a* (0,0,0) as expected. Relatively high *R*-values in case of rudashevskyite are obviously attributed to poor quality of its reflections, in particular of those related to the third domain. This is also a reason for low precision of the cell refinement and significant departure of single-crystal *a* parameters (5.439–5.444 Å) relative to that obtained from powder data (5.426 Å). Low quality of the rudashevskyite pattern is illustrated by Figures 5 and 6 that represent reconstructions of the zero-layer of reciprocal space of the first domain along [001] and [110], respectively. A pronounced streaking of reflections is caused by splintering or bending of the crystals, as illustrated by Figures 2 and 3. Analysis of three-dimensional shapes of reflections along with their orientation in reciprocal space result in the conclusion that rudashevskyite domains are platelets flattened on (111). Contrary to rudashevskyite, the kamacite crystal exhibits sharp and well developed reflections (Fig. 6), and its *a* parameter of 2.866 Å is in excellent agreement with the data on natural kamacite (2.868 Å, Keller et al. 1986).

Schematic projections of rudashevskyite domains onto the cube plane of embedded kamacite crystal are displayed on Figure 7. Investigation of relative orientation of domains (Recipe program from Stoe X-Area package) revealed that they are arranged in a non-random way. The angular distance between nearest [100] axes of the first and second domain is about 11°, between the first and third ~6°, and ~14° between domains 2 and 3. Thus, one

[1] Deposit item AM-08-020, supplementary reflection data. Deposit items are available two ways: For a paper copy contact the Business Office of the Mineralogical Society of America (see inside front cover of recent issue) for price information. For an electronic copy visit the MSA web site at http://www.minsocam.org, go to the American Mineralogist Contents, find the table of contents for the specific volume/issue wanted, and then click on the deposit link there.

TABLE 3. Crystallographic data, refinement parameters and isotropic displacement parameters for rudashevskyite and kamacite

	Rudashevskyite			Kamacite
	Domain 1	Domain 2	Domain 3	
Space group	$F\bar{4}3m$	$F\bar{4}3m$	$F\bar{4}3m$	$Im\bar{3}m$
a (Å)	5.441(8)	5.439(9)	5.444(17)	2.866(5)
a (Å) powder*	5.426(2)	5.426(2)	5.426(2)	
Z	4	4	4	2
μ (mm^{-1})	9.98	9.99	9.97	29.64
Total reflections	365	365	378	119
Unique reflections	38	38	38	7
Unique observed, $\|F_o\| \geq 4\sigma_F$	26	26	23	7
2θ min, max (°)	6.51, 29.35	6.51, 29.35	6.51, 29.35	10.1, 27,65
h,k,l (min)	$\bar{7},\bar{6},\bar{7}$	$\bar{7},\bar{7},\bar{7}$	$\bar{7},\bar{6},\bar{7}$	$\bar{3},\bar{3},\bar{3}$
h,k,l (max)	7,7,7	6,6,7	7,7,7	3,3,3
R_{int}	0.266	0.257	0.474	0.168
R_o	0.094	0.106	0.169	0.042
R_1 ($\|F_o\| \geq 4\sigma_F$)	0.053	0.050	0.106	0.012
R_1 (all)	0.099	0.085	0.170	0.012
wR_2	0.203	0.182	0.245	0.044
S = *GooF*	1.253	1.122	1.101	0.526
U_{iso} for (Fe,Zn)	0.041(2)	0.038(2)	0.041(3)	0.010(2)
U_{iso} for S	0.056(4)	0.046(3)	0.053(5)	

* Value refined from powder data and used in structure refinement.

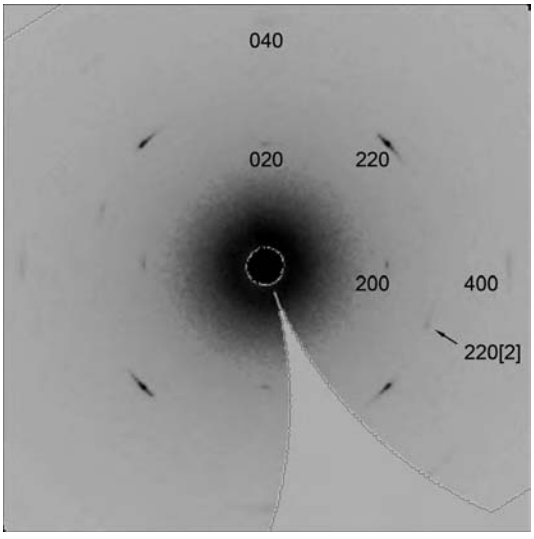

FIGURE 5. Reconstruction of reciprocal space of rudashevskyite (first domain) along [001], zero-layer. Note weak reflections attributed to the second domain [220(2)].

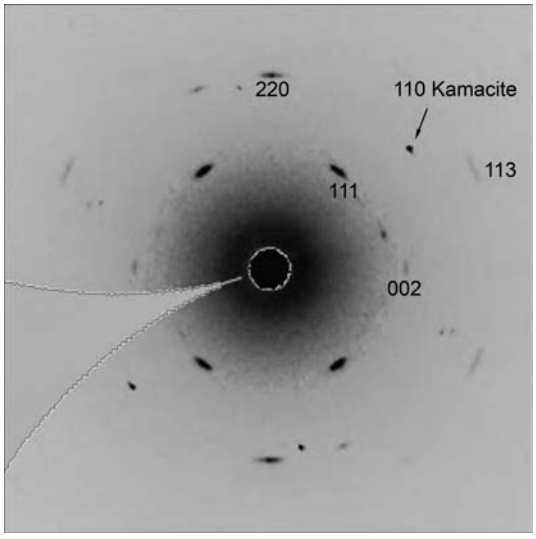

FIGURE 6. Reconstruction of reciprocal space of rudashevskyite (first domain) along [110], zero-layer. Note weak and smeared reflections attributed to the adjacent rudashevskyite domains, and sharp (110) reflections of embedded kamacite crystal (110 Kamacite).

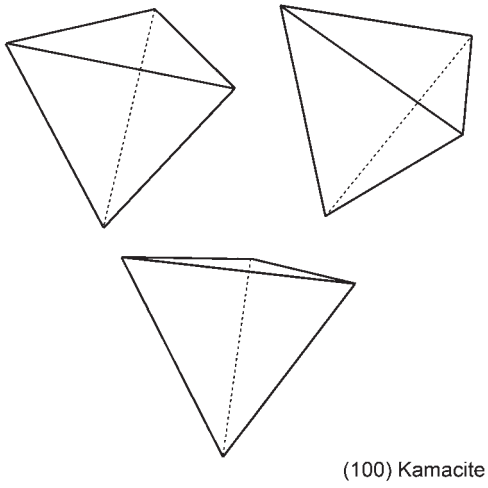

FIGURE 7. Schematic projections of the three rudashevskyite domains (displayed as tetrahedra) onto cube plane of embedded kamacite crystal.

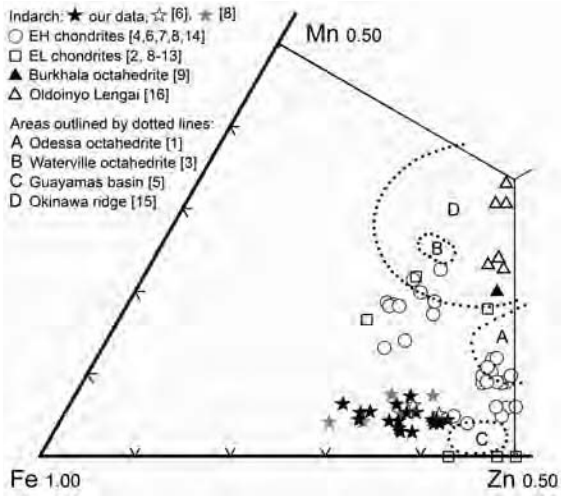

FIGURE 8. Chemical composition of natural Fe-dominant members of FeS-ZnS-MnS system. Scale in apfu (2 apfu total). References: [1] El Goresy (1967); [2] Buseck and Holdsworth (1972); [3] Weinke et al. (1977); [4] Rambaldi et al. (1986); [5] Peter and Scott (1988); [6] El Goresy and Ehlers (1989); [7] Ikeda (1989); [8] Kissin (1989); [9] Yaroshevsky et al. (1989); [10] Lin et al. (1991); [11] Zhang and Sears (1996); [12] Lin and Kimura (1997); [13] Petrichenko and Ulyanov (1998); [14] Lin and El Goresy (2002); [15] Glasby and Notsu (2003); [16] Mitchell and Belton (2004).

can assume that the studied grain is a subparallel intergrowth of the crystals, as illustrated by Figure 2. The average orientation of rudashevskyite domains relative to kamacite may, in turn, be represented as [110] of rudashevskyite is approximately coincident with [111] of kamacite.

Powder diffraction data for rudashevskyite (Table 4) were obtained with a 114.6 mm Debye-Scherrer camera using Mn-filtered Fe*K*α-radiation at 30 kV and 40 mA. Kamacite lines in the powder pattern do not overlap with rudashevskyite lines and were used for internal calibration of the film. Cell parameter *a* was refined by least-squares to 5.426(2) Å, *V* 159.8(2) Å^3, *Z* = 4.

TABLE 4. X-ray powder diffraction data for rudashevskyite compared with TEM data for bacterial cubic FeS (Postfai et al. 1998a)

Rudashevskyite*				Cubic FeS	
I_{obs}	d_{obs}	I_{calc}	d_{calc}	d_{obs}	*h k l*
100	3.130	100	3.133	3.12	1 1 1
10	2.714	9	2.713	2.70	2 0 0
50	1.919	58	1.918	1.91	2 2 0
40	1.634	38	1.636	1.63	3 1 1
		2	1.566	1.56	2 2 2
5	1.359	10	1.357	1.35	4 0 0
30	1.246	19	1.245		3 3 1
		3	1.213		4 2 0
30	1.107	37	1.108		4 2 2
30	1.045	25	1.044		5 1 1
		8	1.044		3 3 3

* Debye-Scherrer 114.6 mm camera, Fe*K*α radiation, Mn filter, 30 kV, 40 mA, visual estimation of intensities, internal standard kamacite.

NATURAL OCCURRENCES OF IRON-DOMINANT ZnS-FeS-MnS MINERALS

Figure 8 summarizes data on the chemical compositions of known (Fe,Zn,Mn)S minerals, both of meteoritic and terrestrial origin. Besides Indarch, Fe-dominant members of FeS-ZnS-MnS solid solutions were found in 11 meteorites related to enstatite chondrites: Yilmia (EL6) (Buseck and Holdsworth 1972); Pillistfer (EL6), ALHA77295 (EH3) (Kissin 1989); MAC88136 (EL3) (Lin et al. 1991); LEW88135 (EL6), MAC88180 (EL3), MAC88184 (EL3) (Zhang and Sears 1996); Yamato-86004 (EH6) (Lin and Kimura 1997); PCA91020 (EL3) (Petrichenko and Ulyanov 1998); Qingzhen (EH3) (Rambaldi et al. 1986; El Goresy et al. 1988; El Goresy and Ehlers 1989; Kissin 1989; Lin and El Goresy 2002); and Yamato-691 (EH3) (El Goresy et al. 1988; Kimura 1988; Ikeda 1989). Other extraterrestrial occurrences include three iron meteorites (octahedrites) related to the IAB chemical group: Odessa (El Goresy 1967), Waterville (Weinke et al. 1977), and Burkhala (Yaroshevsky et al. 1989).

Terrestrial occurrences of (Fe,Zn,Mn)S minerals were reported from hydrothermal assemblages of black smokers in oceanic rift zones: Southern Trough of Guaymas basin, Gulf of California (Peter and Scott 1988), TAG hydrothermal field, Mid-Atlantic Ridge (Lawrie and Miller 2000), and submarine Iheya Ridge, Okinawa Trough, SW of Japan (Izawa et al. 1991; Glasby and Notsu 2003). In addition, Fe-dominant members of this series were described from natrocarbonatite lavas of Oldoinyo Lengai volcano, Tanzania (Mitchell and Belton 2004).

Pósfai et al. (1998a, 1998b) reported on the unusual association of iron sulfides in magnetotactic bacteria, so-called many-celled prokaryotes. Cubic sphalerite-type FeS was tentatively recognized among these sulfides, based on electron diffraction data (their Table 3, Pósfai et al. 1998a) and semi-quantitative EDS analysis. However, this biogenic occurrence of sphalerite-type FeS requires additional study.

SHALERITE-WURTZITE POLYTYPISM AND IMPLICATION TO GEOTHERMOMETRY AND GEOBAROMETRY

There are numerous papers devoted to application of ZnS-FeS system in geothermometry and geobarometry. Experimental investigations of this join were initiated by work of Kullerud (1953), who showed that Fe content in sphalerite may be applied as a geological

thermometer. This was followed by studies of the system under different conditions intended to simulate natural processes. Experiments were carried out both under hydrothermal conditions and in the solid state. In hydrothermally synthesized sphalerites, FeS content may approach as much as 53.5 mol% (Sorokin et al. 1968). The results of syntheses in the solid state proved the existence of a continuous sphalerite-type ZnS-FeS series with up to 56–58 mol% of FeS (Barton and Toulmin 1966; Balabin and Urusov 1995). It has been shown (Barton and Toulmin 1966) that substitution of Fe for Zn stabilizes the wurtzite structure and reduces the temperature of the reversible sphalerite-wurtzite inversion in the solid state from ~1020 °C for pure ZnS to as low as ~850 °C at 56 mol% of FeS. Scott and Barnes (1972) showed that in dry systems, the upper limit for FeS incorporation in sphalerite is dependent on three factors: temperature (direct dependence), pressure and sulfur fugacity (inverse dependence). Sulfur fugacity in the experiments is controlled by the selection of an appropriate type of Fe-S buffer. The highest FeS contents in synthetic sphalerite solid solutions, 56 mol% (Barton and Toulmin 1966) and 58 mol% (Balabin and Urusov 1995), were obtained with the Fe/FeS buffer that is similar to kamacite-troilite assemblage typical of enstatite chondrites and iron meteorites.

Phase relations in the ZnS-FeS-MnS system were also studied by several authors, to establish the influence of Mn and Fe substitution on the sphalerite-wurtzite transformation. Solid-state syntheses (Tauson and Chernyschev 1977, 1978; Tauson et al. 1977; Shima et al. 1982) revealed that Mn and Fe substitution stabilizes the wurtzite structure to as low as 350 °C, with a wide wurtzite stability field around the center of ZnS-FeS-MnS triangle. An extended series of gas-transport syntheses in the ZnS-MnS-FeS system at 800 °C was carried out by Knitter and Binnewies (2000). Their results show that Fe-dominant (Fe,Zn,Mn)S compounds all crystallize in the wurtzite polytype, with Mn as an essential stabilizing constituent. Well-known sphalerite-wurtzite polytypysm is a characteristic feature of FeS-ZnS-MnS solid solutions. Pure MnS may crystallize in both polytypes, hexagonal rambergite-2*H* (Kalinowski 1996) and synthetic cubic MnS-3*C* (Mehmed and Haraldsen 1938). Cubic sphalerite-type FeS is known but it is metastable. This polymorph has been synthesized by de Médicis (1970a, 1970b) and Takeno et al. (1970) as a product of low-temperature iron corrosion in hydrogen sulfide solutions.

Note that until present description, none of meteoritic occurrences of ZnS-FeS-MnS minerals were supported by either X-ray or TEM data, thus their structural nature remains unsolved. In this respect, meteoritic (Fe,Zn,Mn)S minerals, especially their Mn-rich varieties, require additional study to establish their relation to either sphalerite or wurtzite structure—an important point necessary for understanding of meteorite formation. This uncertainty, along with apparent inhomohenity of ZnS-FeS-MnS sulfides in many of chondritic meteorites, leaves a wide field for further investigations.

ACKNOWLEDGMENTS

We thank Sergey Krivovichev for helpful discussions of the manuscript; Anton Antonov and Dmitry Lyalinov for support in microprobe studies. The manuscript was substantially improved by constructive reviews of Ahmed El Goresy, Marcello Mellini, and Paul Barton. The authors are indebted to developers of the libraries of NASA Astrophysics Data System and American Mineralogist Crystal Structure Database, for comprehensive literature selection. Specimen of Sardis meteorite has been kindly provided for study by the Mining Museum, St. Petersburg Mining Institute (Technical University). This work was carried out under support of National educational program "Innovative educational environment in classic University," project "Molecular Geochemistry and Biogeochemistry."

REFERENCES CITED

Balabin, A.I. and Urusov, V.S. (1995) Recalibration of the sphalerite cosmobarometer: Experimental and theoretical treatment. Geochimica et Cosmochimica Acta, 59, 1401–1410.

Barton, Jr., P.B., and Toulmin, III, P. (1966) Phase relations involving sphalerite in the Fe-Zn-S system. Economic Geology, 61, 815–849.

Boldyreva, M.M., Romanovsky, J.V., and Kiselev, D.A. (2002) MicroMin, a software for the identification and calculation of color values of ore minerals (abstract). Mineralogical Museums, IV International Symposium, St. Petersburg, p. 358–359 (in Russian).

Brearley, A.J. and Jones, R.H. (1998) Chondritic meteorites. In J.J. Papike, Ed., Planetary Materials, 36, p. 313–398. Reviews in Mineralogy, Mineralogical Society of America, Chantilly, Virginia.

Buseck, P.R. and Holdsworth, E.F. (1972) Mineralogy and petrology of the Yilmia enstatite chondrite. Meteoritics, 7, 429–447.

Chen, M., Shu, J., Xie, X., and Mao, H. (2003) Natural $CaTi_2O_4$-structured $FeCr_2O_4$ polymorph in the Suizhou meteorite and its significance in mantle mineralogy. Geochimica et Cosmochimica Acta, 67, 3937–3942.

Chvileva, T.N., Bezsmertnaya, M.S., Spiridonov, E.M., Agroskin, A.S., Papayan, G.V., Vinogradova, R.A., Lebedeva, S.I., Zavyalov, E.N., Filimonova, A.A., Petrov, K.K., Rautian, L.P., and Sveshnikova, O.L. (1988) Handbook for determination of ore minerals in reflected light, 504 p. Nedra, Moscow (in Russian).

Criddle, A.J. and Stanley, C.J. (1993) Quantitative data file for ore minerals, 3rd edition, 635 p. Chapman and Hall, London.

de Médicis, R. (1970a) Une nouvelle forme de sulfure de fer. Revue de Chimie Minérale, 7, 723–728.

——— (1970b) Cubic FeS, a metastable iron sulfide. Science, 170, 1191–1192.

El Goresy, A. (1967) Quantitative electron microprobe analyses of coexisting sphalerite, daubreelite, and troilite in the Odessa iron meteorite and their genetic implications. Geochimica et Cosmochimica Acta, 31, 1667–1676.

El Goresy, A. and Ehlers, K. (1987) Sphalerite relations in EH-chondrites: Textures, compositions, diffusion profiles and their relevance to temperature and pressure history (abstr.). Meteoritics, 22, 370–371.

——— (1989) Sphalerites in EH chondrites: I. Textural relations, compositions, diffusion profiles, and pressure-temperature histories. Geochimica et Cosmochimica Acta, 53, 1657–1668.

El Goresy, A., Yabuki, H., Ehlers, K., Woolum, D., and Pernicka, E. (1988) Qingzhen and Yamato-691: A tentative alphabet for the EH chondrites. Proceedings of 1st National Institute of Polar Research Symposium on Antarctic Meteorites, 65–101.

Glasby, G.P. and Notsu, K. (2003) Submarine hydrothermal mineralization in the Okinawa Trough, SW of Japan: An overview. Ore Geology Reviews, 23, 299–339.

Ikeda, Y. (1989) Petrochemical study of the Yamato-691 enstatite chondrite (EH3) IV: Descriptions and mineral chemistry of opaque nodules. Proceedings of NIPR Symposium on Antarctic Meteorites, 2, 109–146.

Izawa, E., Motomura, Y., Tanaka, T., and Kimura, M. (1991) Hydrothermal carbonate chimneys in the Iheya Ridge of the Okinawa Trough. JAMSTECTR Deep-Sea Research, 7, 185–192.

Kalinowski, M.P. (1996) Rambergite, a new polymorph of MnS with hexagonal structure. Geologiska Föreningens i Stockholm Förhandligar, 118, A53–A54.

Keller, L., Rask, J., and Buseck, P. (1986) Kamacite, file 37–474. ICDD Powder Diffraction File.

Kimura, M. (1988) Origin of the opaque minerals in an unequilibrated enstatite chondrite, Yamato-691. Proceedings of NIPR Symposium on Antarctic Meteorites, 1, 51–64.

Kissin, S.A. (1986) Application of the sphalerite cosmobarometer to the enstatite chondrites (abstract). Meteoritics, 21, 417–418.

——— (1989) Application of the sphalerite cosmobarometer to the enstatite chondrites. Geochimica et Cosmochimica Acta, 53, 1649–1655.

Knitter, S. and Binnewies, M. (2000) Chemical vapor transport of solid solutions. Part 7. Chemical transport of FeS/MnS/ZnS mixed crystals. Zeitschrift für Anorganische und Allgemeine Chemie, 626, 2335–2339.

Kullerud, G. (1953) The FeS-ZnS system, a geological thermometer. Norsk Geologisk Tidsskrift, 32, 61–147.

Lawrie, D. and Miller, D.J. (2000) Data Report: Sulfide mineral chemistry and petrography from Bent Hill, ODP mound, and TAG massive sulfide deposits. In R.A. Zierenberg, Y. Fouquet, D.J. Miller, and W.R. Normark, Eds., Proceedings of the Ocean Drilling Program. Scientific Results, 169, 34 p.

Lin, Y. and Kimura, M. (1997) Thermal histories and parent body(ies) of EH chondrites: Evidences from new highly equilibrated EHs (Y793225, 82189, 8404, 8414 and 86004). Lunar and Planetary Science, XXVIII, abstract 1130.

——— (1998) Petrographical and mineral chemical study of new EH melt rocks

and a new grouplet of enstatite chondrites. Meteoritics and Planetary Science, 33, 501–511.
Lin, Y.T. and El Goresy, A. (2002) A comparative study of opaque phases in Qingzhen (EH3) and MacAlpine Hills 88136 (EL3): Representatives of EH and EL parent bodies. Meteoritics and Planetary Science, 37, 577–599.
Lin, Y.T., Nagel, H-J., Lindberg, L.L., and El Goresy, A. (1991) MAC88136—the first EL3 chondrite. Lunar and Planetary Science, XXII, abstract 811.
Lorenz, C., Kurat, G., Brandstätter, F., and Nazarov, M.A. (2003) NWA 1235: A phlogopite-bearing enstatite meteorite. Lunar and Planetary Science, XXIV, abstract 1211.
Mehmed, F. and Haraldsen, H. (1938) Das magnetische Verhalten der allotropen Modifikationen des Mangan(II)-Sulfides. Zeitschrift für Anorganische und Allgemeine Chemie, 235, 193–200.
Mitchell, R.H. and Belton, F. (2004) Niocalite-cuspidine solid solution and manganoan monticellite from natrocarbonatite, Oldoinyo Lengai, Tanzania. Mineralogical Magazine, 68, 787–799.
Murowchick, J.B. and Barnes, H.L. (1986) Formation of cubic FeS. American Mineralogist, 71, 1243–1246.
Nagel, H.-J., Lin, Y.T., and El Goresy, A. (1989) Sphalerite compositions in meteorites: A dilemma of an originally promising cosmobarometer. Meteoritics, 24, 307 (abstract).
Peter, J.M. and Scott, S.D. (1988) Mineralogy, composition, and fluid-inclusion microthermometry of seafloor hydrothermal deposits in the Southern Through of Guaymas basin, Gulf of California. Canadian Mineralogist, 26, 567–587.
Petrichenko, A.S. and Ulyanov, A.A. (1998) Enstatite chondrite PCA91020—opaque minerals and revision of classification. Lunar and Planetary Science, XXIX, abstract 1381.
Pósfai, M., Buseck, P.R., Bazylinski, D.A., and Frankel, R.B. (1998a) Reaction sequence of iron sulfide minerals in bacteria and their use as biomarkers. Science, 280, 880–883.
——— (1998b) Iron sulfides from magnetotactic bacteria: Structure, composition, and phase transitions. American Mineralogist 83, 1469–1481.
Rambaldi, E.R., Rajan, R.S., Housley, R.M., and Wang, D. (1986) Gallium-bearing sphalerite in metal-sulphide nodules of the Quingzhen (EH3) chondrite. Meteoritics, 21, 23–32.
Ramdohr, P. (1963) The opaque minerals in stony meteorites. Journal of Geophysical Research, 68, 2011–2036.
——— (1973) The Opaque Minerals in Stony Meteorites, 245 p. Elsevier, New York.
Schwarcz, H.P., Scott, S.D., and Kissin, S.A. (1975) Pressures of formation of iron meteorites from sphalerite compositions. Geochimica et Cosmochimica Acta, 39, 1457–1466.
Scott, S.D. and Barnes, H.L. (1972) Sphalerite—wurtzite equilibria and stoichiometry. Geochimica et Cosmochimica Acta, 36, 1275–1295.
Sheldrick, G.M. (1997) SHELXL-97, Program for the Refinement of Crystal Structures, Universität Göttingen, Germany.
Shima, H., Ueno, H., and Nakamura, Y. (1982) Synthesis and phase studies on sphalerite solid solution—the systems Cu-Fe-Zn-S and Mn-Fe-Zn-S. Journal of Japanese Association of Mineralogy, Petrology and Economic Geology, Spec. Issue 3, 271–280 (in Japanese, English Abstract).
Sorokin, V.I., Gruzdev, V.S., and Shorygin, V.A. (1968) Changes in lattice parameter a of sphalerite, produced under hydrothermal conditions, as a function of its iron content. In I. Ya. Nekrasov Ravnovesii, Ed., Eksperimental'nie i Teoreticheskie Issledovaniya Mineral'nih, 113–116. Nauka, Moscow (in Russian).
Takeno, S., Zoka, H., and Niihara, T. (1970) Metastable cubic iron sulfide—with special reference to mackinawite. American Mineralogist, 55, 1639–1649.
Tauson, V.L. and Chernyschev, L.V. (1977) Phase relations and structural features of ZnS-MnS mixed crystals. Geochemistry International, 14, 11–22.
——— (1978) The sphalerite-wurtzite transition in isomorphous mixtures of the system ZnS-MnS-CdS-FeS. Geochemistry International, 15, 33–41.
Tauson, V.L., Chernyshev, L.V., and Makeyev, A.B. (1977) Phase relations and structural characteristics of mixed crystals in the system ZnS-MnS. Geochemistry International, 14, 33–45.
Weinke, H.H., Kiesl, W., and Clarke, Jr., R.S. (1977) Mineralogical and chemical investigation of the Waterville iron meteorite. Meteoritics, 12, 561–564.
Yaroshevsky, A.A., Migdisova, L.F., and Kononkova, N.N. (1989) Mineral associations of sulfide nodules of iron meteorite Burkhala and conditions of its formation. Geokhimiya, 6, 825–837 (in Russian).
Zhang, Y. and Sears, D.W.G. (1996) The thermometry of enstatite chondrites: a brief review and update. Meteoritics and Planetary Science, 31, 647–655.

MANUSCRIPT RECEIVED JANUARY 29, 2007
MANUSCRIPT ACCEPTED DECEMBER 18, 2007
MANUSCRIPT HANDLED BY PAOLA BONAZZI